Preparation and Characterisation of Mg–Al Layered Double Hydroxides Intercalated with 2-Naphthalene Sulphonate and 2,6-Naphthalene Disulphonate

Tomohito Kameda*, Masami Saito and Yoshiaki Umetsu

Institute of Multidisciplinary Research for Advanced Materials (IMRAM), Tohoku University, Sendai 980-8577, Japan

A Mg–Al layered double hydroxide (Mg–Al LDH) has been modified with aromatic anions by a coprecipitation technique. This method is based on the anion-exchange characteristics of the hydrotalcite-type compound which intercalates various anions, including anions of organic acids, in the interlayer. The Mg–Al LDHs are intercalated with 2-naphthalene sulphonate (2-NS$^-$) and 2,6-naphthalene disulphonate (2,6-NDS^{2-}) ions, which contain a naphthalene ring with one and two sulphonate ($-SO_3^-$) groups in their structures, respectively. They are formed by the dropwise addition of a mixed aqueous solution of $Mg(NO_3)_2$ and $Al(NO_3)_3$ (Al/Mg mole ratio = 1/3) to a solution containing the individual organic anion at a constant pH of 10.0. The Mg–Al LDHs modified with aromatic anion are expected to recognize and selectively uptake hazardous aromatic compounds, such as bisphenol A, from aqueous solutions. The composite materials prepared were characterized by X-ray diffraction, FT-IR spectroscopy and chemical analyses.

2-NS$^-$ was observed to be intercalated into the interlayer almost fully up to the accommodation expected based on the neutralisation of the positive charge of the host lattice. The intercalation of 2,6-NDS^{2-} was approximately 80% of the expected value, however. IR analysis results show that the organic anions are intercalated into the Mg–Al LDH without any significant change in their intrinsic structure.

The X-ray diffraction data suggest that the intercalation of the organic anions under consideration was accompanied by an expansion in the basal spacing of the LDHs. The X-ray diffraction patterns of the 2-NS$^-$-modified LDH suggested the formation of two types of LDHs showing different basal spacing at higher 2-NS$^-$ content. On the other hand, the 2,6-NDS$^-$-modified LDH showed diffraction peaks, which corresponded to the basal spacing, with widely spreading peak angles and reduced intensity, suggesting the widely varying basal spacing of the Mg–Al LDH.

1. Introduction

Mg–Al layered double hydroxide (Mg–Al LDH: $[Mg^{2+}_{1-x}Al^{3+}_x(OH)_2](A^{n-})_{x/n} \cdot mH_2O$) is widely recognized as a clay mineral exhibiting an anion exchange property.[1–3] The host lattice of the layer-structured crystal consists of brucite ($Mg(OH)_2$)-like octahedral layers that are positively charged due to the replacement of Mg atoms by Al atoms. The positive charge of the host lattice is neutralised by the intercalated anions in the interlayers, and its remaining space is occupied by water molecules. Mg–Al LDH can intercalate various types of inorganic anions, such as AsO_4^{3-}, Cl^-, NO_3^-, F^-, SO_4^{2-}, CO_3^{2-}, BO_3^{3-} and HPO_4^{2-} in its interlayers.[4–13] Similarly, the intercalation of organic anions, such as phenols, anionic surfactants and coloured organics, in the interlayer of Mg–Al LDH has been investigated from various viewpoints.[14–18] The organic-inorganic composites produced by intercalation of organic acid anions in the interlayer of Mg–Al LDH are expected to perform various functions due to the functional groups of the organic acid anions.[19,20]
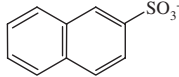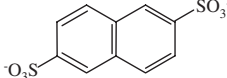
Our previous paper has described the preparation of Mg–Al LDH particles modified with dodecylsulfate ions (DS$^-$) as well as their behaviour during bisphenol A elimination.[19] The Mg–Al LDH (Mg/Al mole ratio: 3.0) was prepared by intercalating DS$^-$ in the interlayer of Mg–Al LDH; further, it was observed that the Mg–Al LDH exhibits a capacity for the uptake of bisphenol A in aqueous solution. This function of the composite material was caused largely due to the hydrophobic interactions between the intercalated DS$^-$ and bisphenol A.[19]

However, the DS$^-$-modified Mg–Al LDH is unable to distinguish the target organic material from other organic species coexisting in aqueous solutions. In the environment, various types of hazardous organic contaminants coexist with other organic materials in effluents and wastewaters. Therefore, it is desired in water-treatment processes that the composite material is capable of the selective uptake for a target organic contaminant. Generally, it is known that the aromatic ring is activated by the electron-donating groups in the molecular structure of the aromatic compound, and the aromatic ring is deactivated by the electron-accepting groups of the aromatic compound. The activated aromatic ring bears a potential to interact with the deactivated aromatic ring to generate a π–π stacking. Therefore, the Mg–Al LDH modified with aromatic anions is expected selectively to take out the organic materials bearing an aromatic ring from environmental water through this π–π stacking interaction.

For the purpose mentioned above, we have attempted to prepare Mg–Al LDHs modified with 2-naphthalene sulphonate (2-NS$^-$) and 2,6-naphthalene disulphonate (2,6-NDS^{2-}) ions that include aromatic rings in their structures, as shown in Table 1. As shown in Fig. 1(a), 2-NS$^-$ contains an electron-accepting $-SO_3^-$ group in its structure. Therefore, it is assumed that a part of the naphthalene ring of 2-NS$^-$ is deactivated by the $-SO_3^-$ group, and the part of the ring far from the $-SO_3^-$ group is in an activated state. When Mg–Al LDH is modified with 2-NS$^-$, the composite material is expected to exhibit an uptake capacity for organic materials containing either activated or deactivated aromatic rings. On the other hand, 2,6-NDS^{2-} contains two $-SO_3^-$ groups at the sites of 2 and 6 in the naphthalene ring, and the entire naphthalene ring is deactivated as shown in Fig. 1(b). Therefore, Mg–Al LDH modified with 2,6-NDS^{2-} is ex-

*Corresponding author, E-mail: kameda@tagen.tohoku.ac.jp

Table 1   Chemical formulae and structures of 2-naphthalene sulphonate and 2,6-naphthalene disulphonate ions.

	Chemical formula	Structure
(a) 2-naphthalene sulphonate ion (2-NS$^-$)	$C_{10}H_7O_3S^-$	
(b) 2,6-naphthalene disulphonate ion (2,6-NDS^{2-})	$C_{10}H_6O_6S_2^{2-}$	

(a)   (b)
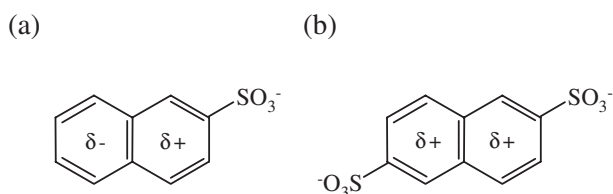
Fig. 1   Electronic state of (a) 2-NS$^-$ and (b) 2,6-NDS^{2-}.

pected to interact selectively with the organic material bearing an activated aromatic ring. This paper will describe the preparation of Mg–Al LDHs modified with 2-NS$^-$ and 2,6-NDS^{2-} as well as their features examined by the X-ray diffraction (XRD) and Fourier transform infrared spectroscopy (FT-IR) analyses.
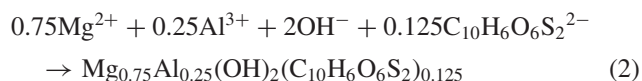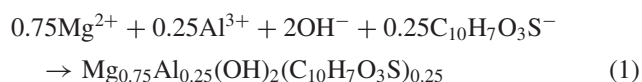
2.   Experimental

All the reagents used were of chemical reagent grade (Wako Pure Chemical Industries, Ltd., Japan). The water used in this study was purified by distillation and further deionisation using ADVANTEC AQUARIUS GS-20R to the electric resistivity of 0.05 μS level. In this paper, the units of volume, concentration, time, and temperature are expressed by l (dm^3), mol/L (kmol/m^3), min (60 s), h (3600 s), and °C (θ + 273.15 K), respectively.

2.1   Preparation

The Mg–Al solution (0.15 mol/L Mg(NO$_3$)$_2$ + 0.05 mol/L Al(NO$_3$)$_3$, the Mg/Al mole ratio of 3.0) was prepared by dissolving Mg(NO$_3$)$_2$·6H$_2$O (37.5 mmol) and Al(NO$_3$)$_3$· 9H$_2$O (12.5 mmol) in 250 mL of deionised water. The solutions of 2-naphthalenesulphonic acid sodium salt (2-NS–Na) were prepared by dissolving a required amount of C$_{10}$H$_7$SO$_3$Na in 250 mL of a mixture solution of ethanol and deionised water at a volume ratio of 1:1. The ethanol–water mixture solution has a sufficient solubility for 2-NS–Na, which is sparingly soluble in water. The solutions of 2,6-naphthalenedisulphonic acid disodium salt (2,6-NDS–Na$_2$) were prepared by dissolving a required amount of C$_{10}$H$_6$(SO$_3$Na)$_2$ in 250 mL of deionised water.

2-NS·Mg–Al LDHs (theoretical formula: Mg$_{0.75}$Al$_{0.25}$-(OH)$_2$(C$_{10}$H$_7$SO$_3$)$_{0.25}$) and 2,6-NDS·Mg–Al LDHs (theoretical formula: Mg$_{0.75}$Al$_{0.25}$(OH)$_2$(C$_{10}$H$_6$(SO$_3$)$_2$)$_{0.125}$) were prepared by dropwise addition of the Mg–Al solution to the 2-NS–Na solution and the 2,6-NDS–Na$_2$ solution, respectively, at a constant pH of 10.0. The co-precipitation reaction can be expressed by either eq. (1) or (2), where the

stoichiometric coefficients of 0.25 for 2-NS$^-$ and of 0.125 for 2,6-NDS^{2-}, is calculated based on the neutralisation of the positive electric charge of the Al-bearing brucite-like octahedral layers. This charge arises due to the replacement of Mg atoms by Al at an Mg/Al mole ratio of 3.0.

$$0.75Mg^{2+} + 0.25Al^{3+} + 2OH^- + 0.25C_{10}H_7O_3S^-$$
$$\rightarrow Mg_{0.75}Al_{0.25}(OH)_2(C_{10}H_7O_3S)_{0.25} \quad (1)$$
$$0.75Mg^{2+} + 0.25Al^{3+} + 2OH^- + 0.125C_{10}H_6O_6S_2^{2-}$$
$$\rightarrow Mg_{0.75}Al_{0.25}(OH)_2(C_{10}H_6O_6S_2)_{0.125} \quad (2)$$

The Mg–Al solution, 2-NS–Na solution, and 2,6-NDS–Na$_2$ solution were bubbled with nitrogen gas (N$_2$) for 20 min in order to eliminate the dissolved CO$_2$ for minimising the intercalation of CO$_3^{2-}$. The Mg–Al solution was added dropwise to the 2-NS–Na solution and the 2,6-NDS–Na$_2$ solution, respectively in a closed vessel at a steady rate of 10 mL/min at 30°C under mild agitation. The solution pH was adjusted to 10.0 by addition of 0.5 mol/L NaOH solution using a pH-stat. After the addition of the Mg–Al solution, the resultant suspension was kept standing at 30°C for 1 h. The 2-NS·Mg–Al LDH and 2,6-NDS·Mg–Al LDH crystals were recovered by filtering the resultant suspensions, followed by repeatedly washing of the crystals with deionised water and then drying under a reduced pressure (133 × 10^{-1} Pa) for 40 h. N$_2$ gas was also bubbled into the solutions throughout the coprecipitation operation to minimise the effects due to the dissolved CO$_2$.

In order to confirm that the prepared 2-NS·Mg–Al LDH and 2,6-NDS·Mg–Al LDH had the Mg–Al LDH structures, CO$_3^{2-}$-intercalated Mg–Al LDH (CO$_3$·Mg–Al LDH) has been used as reference material. The CO$_3$·Mg–Al LDH with an Mg/Al mole ratio of 3.0 was prepared by the coprecipitation method in an alkaline carbonate solution as described in detail in our previous paper.[20]

2.2   Characterisation methods

The 2-NS·Mg–Al LDHs, 2,6-NDS·Mg–Al LDHs and CO$_3$·Mg–Al LDH crystals were ground to powders using pestle and mortar, and the resultant powders were identified by XRD using a Rigaku RINT 2200 diffractometer with CuKα radiation at 36 kV and 20 mA (scanning rate of 3°/min). In order to examine the formation of the LDH structure and the presence of 2-NS$^-$ and 2,6-NDS^{2-} in the particles, the infrared spectra of 2-NS·Mg–Al LDHs, 2,6-NDS·Mg–Al LDHs, CO$_3$·Mg–Al LDH, 2-NS–Na and 2,6-NDS–Na$_2$ were measured with a Bio-Rad FTS-45A spectrometer using the KBr disk method. The KBr pellets were prepared by intimately mixing the samples with KBr powders, and the

Table 2 Element analyses and mole ratios of Mg/Al and 2-NS/Al for 2-NS·Mg–Al LDHs prepared from solutions with 2-NS/Al mole ratios of 0.5, 1.0 and 2.0.

2-NS/Al mole ratio in solution	mass%			mole ratio	
	Mg	Al	2-NS	Mg/Al	2-NS/Al
0.5	15.4	5.9	19.3	2.9	0.43
1.0	16.6	6.3	39.6	2.9	0.82
2.0	14.1	5.4	40.0	2.9	0.96

content of the samples in the KBr pellets was fixed at the w/w ratio of 0.5%.

The first step in the chemical analysis of the 2-NS·Mg–Al LDHs was the dissolution of the samples in 1 mol/L HCl–ethanol solution. In this case, the ethanol–water solution was used to dissolve the Mg or Al salt of 2-NS$^-$ produced in the course of the dissolution of Mg–Al LDH by HCl. The 2-NS$^-$ present in the solutions was analysed spectrometrically at a wavelength of 275 nm. The high concentration of ethanol in the solution severely hampered the analysis of Mg and Al by inductively coupled plasma-atomic emission spectroscopy (ICP-AES). The Al concentration in the solution was then determined by EDTA-back-titrimetric method at pH 5–6 using a Zn standard solution and a xylenol orange indicator.[21] Mg could not be determined even by this method since a colour change of the indicator was not clearly observed under the conditions in this study. Therefore, the Mg/Al mole ratios in the 2-NS·Mg–Al LDHs were first determined by X-ray fluorescence (XRF) analysis, and then the Mg contents were calculated based on the analysed Al concentration. On the other hand, 2,6-NDS·Mg–Al LDH is soluble in aqueous HCl solution without ethanol. The 2,6-NDS·Mg–Al LDHs were dissolved in 1 mol/L HCl solution, and the 2,6-NDS^{2-} present in the solutions was analysed spectrometrically at a wavelength of 275 nm. The 2,6-NDS·Mg–Al LDHs were also dissolved in 6 mol/L HNO$_3$ solution for analysis of Mg and Al using ICP-AES.

3. Results and Discussion

3.1 Preparation of 2-NS·Mg–Al LDH

The 2-NS·Mg–Al LDHs were prepared by a coprecipitation technique, which involved the dropwise addition of the Mg–Al solution to the 2-NS–Na solution at a controlled pH of 10.0. The effect of the concentration of 2-NS$^-$ on its intercalation in the LDH interlayer was examined for the specimen prepared using the 2-NS–Na solutions of three different initial concentrations. They were 0.5, 1.0 and 2.0 times as much as the stoichiometric quantity required by eq. (1), *i.e.*, 2-NS/Al mole ratio = 0.5, 1.0, and 2.0.

Table 2 shows the results of element analyses and calculated mole ratios of Mg/Al and 2-NS/Al in 2-NS·Mg–Al LDHs prepared. In every sample, the Mg/Al mole ratio was 2.9 and very close to the value of 3.0 expected for the preparation procedure in this study. On the other hand, the 2-NS/Al mole ratio increased with increasing 2-NS/Al mole ratio in the solution. The 2-NS/Al mole ratios in 2-NS·Mg–Al LDHs were approximately 80% of the expected values at 0.5 and 1.0 of the 2-NS/Al mole ratio of the solution. Even when the initial concentration of 2-NS$^-$ was
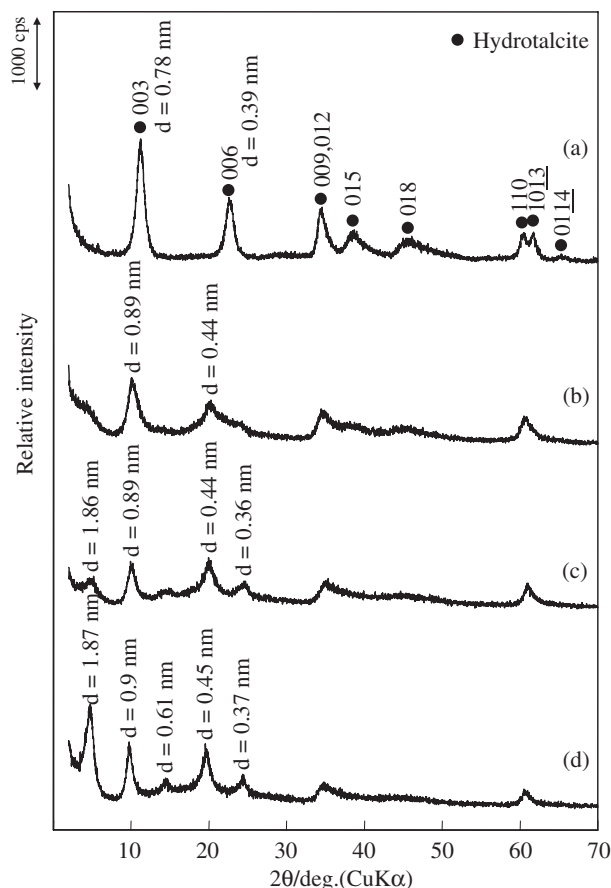

Fig. 2 XRD patterns of (a) CO$_3$·Mg–Al LDH, and 2-NS·Mg–Al LDHs prepared from solutions with 2-NS/Al mole ratios of (b) 0.5, (c) 1.0 and (d) 2.0.

sufficiently high—(twice the stoichiometric concentration)—the 2-NS/Al mole ratio in the LDH was 0.96. These results suggest that the content of 2-NS$^-$ in the LDH was governed primarily by the electric charge balance in Mg–Al LDH without the additional pick-up of 2-NS$^-$ in the interlayer observed for DS$^-$.[19] In the intercalation of DS$^-$, the DS$^-$ content over the DS/Al ratio of 1.0 suggests the uptake of the DS$^-$ by a process other than electric charge balance, such as organic–organic dissolution.[19]

Figure 2 shows the XRD patterns of (a) CO$_3$·Mg–Al LDH as a reference material, and 2-NS·Mg–Al LDHs prepared from solutions with 2-NS/Al mole ratios of (b) 0.5, (c) 1.0 and (d) 2.0. The XRD peaks of CO$_3$·Mg–Al LDH are ascribed to hydrotalcite (JCPDS card 22–700), a hydroxycarbonate of magnesium and aluminum represented as Mg$_6$Al$_2$(OH)$_{16}$CO$_3$·4H$_2$O, which occurs in nature and is a layer-structured double hydroxide. Since the XRD peaks of

LDH are generally indexed on the basis of a hexagonal unit cell, the basal spacing of LDH is equivalent to $1/n^{\text{th}}$ of the c parameter, where n is the number of the layer repeat of the unit cell.[22] The basal spacing is composed of an Al-bearing brucite-like octahedral layer whose thickness and interlayer spacing are affected by the size and orientation of the interlayer anion. Based on the XRD patterns, the basal spacing in the $CO_3 \cdot$Mg–Al LDH was calculated as 0.78 nm. Assuming the brucite-like layer thickness of approximately 0.48 nm as reported by Miyata,[23] the interlayer spacing is calculated to be 0.3 nm. This value is in good agreement with the spacing of the $CO_3 \cdot$Mg–Al LDH reported by Miyata *et al.*[24] It was confirmed that the procedure employed in this study produces an LDH crystal with a well-defined structure.

The XRD peaks of 2-NS$\cdot$Mg–Al LDHs for 2θ greater than 30°, shown in the patterns (b), (c) and (d), were broader in comparison with those for $CO_3 \cdot$Mg–Al LDH. These peaks were ascribed to the hydrotalcite structure possessing a smaller lattice distance, indicating that the basic structures of 2-NS$\cdot$Mg–Al LDHs were quite similar to Mg–Al LDH. In the XRD patterns of (b), the d_{003} and d_{006} peaks of $CO_3 \cdot$Mg–Al LDH shifted from 11.3° and 22.8° to around 10° and 20° (2θ), respectively, suggesting the basal spacing expansion. This indicates that, in the sample prepared by using the solution with a 2-NS/Al mole ratio of 0.5, the basal spacing for Mg–Al LDH expanded approximately from 0.78 to 0.89 nm. This possibly resulted from the intercalation of anions whose size is larger than CO_3^{2-} in the interlayer of Mg–Al LDH. In the XRD patterns of (b), shoulder peaks were observed at around 5° and 24° (2θ). They were featured in the XRD spectra (b), (c) and (d) as two sets of diffraction peaks in the lower 2θ range. One set consists of the peaks at 2θ values of 10° and 20°, corresponding to the basal spacing of the first type of composite $d = 0.9$ and 0.4 nm, respectively. These peaks were observed in the spectra (b) to (d) and remained almost invariant at the peak intensity of the spectra (c) and (d). The other set consists of the peaks at 2θ values of 5°, 15° and 24° corresponding to the basal spacing $d = 1.87$, 0.61 and 0.37 nm, respectively. These peaks increased in the intensity and were sharpened with an increase in the 2-NS/Al mole ratio of the solution. These results suggest the generation of another 2-NS$\cdot$Mg–Al LDH phase that has a well-ordered and expanded basal spacing with a d_{00l} of approximately 1.9 nm at the increased 2-NS/Al mole ratio in 2-NS$\cdot$Mg–Al LDH. Consequently, 2-NS$\cdot$Mg–Al LDH is assumed to exist in two different states with basal spacings of approximately 1.9 and 0.9 nm, suggesting that 2-NS$^-$ in the LDH has been configured in two different modes. This will be discussed later.

Figure 3 shows the FT-IR spectra of the 2-NS$\cdot$Mg–Al LDHs produced at different 2-NS/Al mole ratios in the solutions together with (a) $CO_3 \cdot$Mg–Al LDH, (b) 2-NS–Na. The FT-IR spectra of 2-NS$\cdot$Mg–Al LDHs showed absorption bands characteristic to $CO_3 \cdot$Mg–Al LDH; they are ascribed to the metal-oxygen vibration (500–1000 cm^{-1}) and the H-bonding stretching vibrations of the OH$^-$ group (the large absorption band centered at 3500 cm^{-1}). This observation supports the XRD result that 2-NS$\cdot$Mg–Al LDHs have Mg–Al LDH lattice structures. Further, the FT-IR spectra of the 2-NS$\cdot$Mg–Al LDHs displays the absorption bands detected for
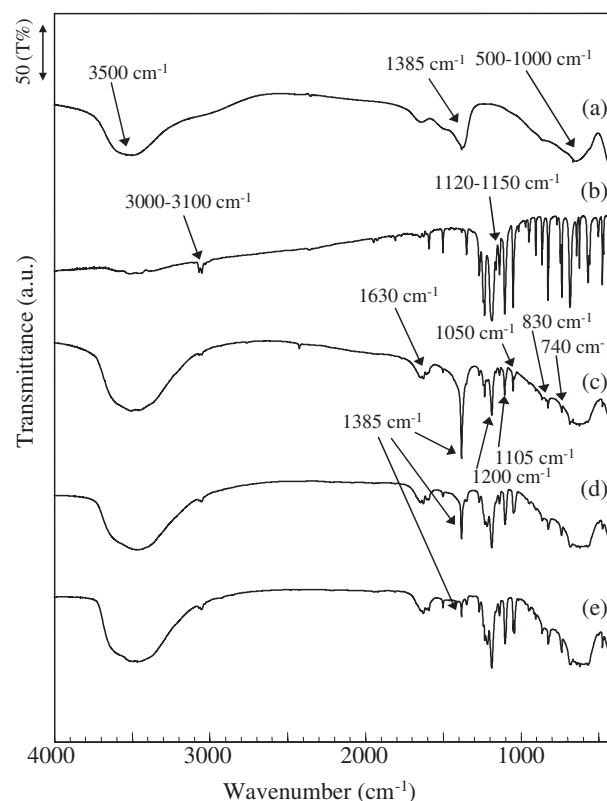

Fig. 3   FT-IR spectra of (a) $CO_3 \cdot$Mg–Al LDH, (b) 2-NS–Na and 2-NS$\cdot$Mg–Al LDHs prepared from solutions with 2-NS/Al mole ratios of (c) 0.5, (d) 1.0 and (e) 2.0.

(b) 2-NS–Na, which correspond to the C–H stretching vibrations in the naphthalene ring (3000–3100 cm^{-1}) and the stretching vibrations of the SO$_2$ group (1120–1150 cm^{-1}). The absorption bands characteristic to 2-NS–Na do not display a detectable shift. These observations demonstrate that the 2-NS$\cdot$Mg–Al LDHs are comprised of an Mg–Al LDH and 2-NS$^-$ with the intrinsic structure unchanged. In addition, the FT-IR spectra of the 2-NS$\cdot$Mg–Al LDHs display an absorption band at 1385 cm^{-1}, which has a different peak shape when compared with an absorption band at around 1385 cm^{-1} in the spectrum of $CO_3 \cdot$Mg–Al LDH. This absorption band is not obviously derived from NO_3^- despite of the preparation of 2-NS$\cdot$Mg–Al LDH in nitrate solution, because J. T. Kloprogge *et al.* report that FT-IR spectrum derived from NO_3^- of NO_3^--intercalated Mg–Al LDH sharply appears at 1360 cm^{-1}.[25] Taking account of the preparation of 2-NS$\cdot$Mg–Al LDH in a highly alkaline solution under a nitrogen atmosphere, the absorption band probably appears due to the O–H bending vibration in OH$^-$. Therefore, OH$^-$ is also considered to be intercalated in the interlayers of 2-NS$\cdot$Mg–Al LDHs. The intercalation of anions other than 2-NS$^-$ is supported by the fact that the 2-NS/Al mole ratios in the LDHs were less than the expected value, as shown in Table 2. In the spectra of (c), (d) and (e), the absorption bands at around 3500 and 1630 cm^{-1} derived from the OH$^-$ group in the host layers and interlayer water remained nearly unchanged in intensity. They were independent of the increase in the 2-NS/Al mole ratio of the sample species, thus reflecting the stability of the Mg–Al
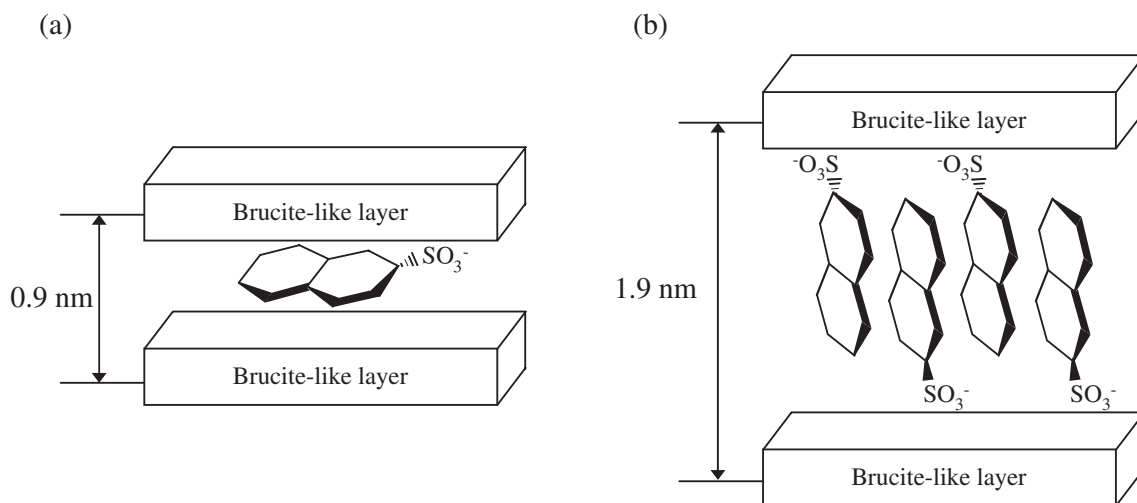
(a)

(b)

Fig. 4   Orientation of the naphthalene ring of 2-NS⁻ along a direction (a) parallel and (b) perpendicular to the brucite-like layers of 2-NS·Mg–Al LDH.

LDH lattice. With an increase in the 2-NS/Al mole ratio, the intensities of the absorption bands at around 1200, 1105, 1050, 830 and 740 cm⁻¹ due to 2-NS⁻ increased; however, the intensity of the absorption band at 1385 cm⁻¹ due to OH⁻ decreased. This leads to a consideration that the intercalation of the 2-NS⁻ takes a place of OH⁻ in the interlayer of 2-NS·Mg–Al LDH at an increased concentration of 2-NS⁻ of the solution.

From the XRD patterns of 2-NS·Mg–Al LDHs in Fig. 2, it is considered that the 2-NS⁻ is intercalated first along an orientation that corresponds to a basal spacing of 0.9 nm. Furthermore, an increasing 2-NS/Al mole ratio in the LDH gives rise to another type of orientation of 2-NS⁻, which corresponds to a basal spacing of 1.9 nm. Assuming the brucite-like layer thickness of 0.48 nm,[23] the interlayer spacings are roughly estimated to be approximately 0.4 and 1.4 nm, respectively. On the other hand, the molecular structure of 2-NS⁻ contains a planar-structured naphthalene ring, and the molecular size in the direction perpendicular to the planar structure is determined by the size of the $-SO_3^-$ group. By considering bond length value of S–O as 0.15 nm, covalent radius of O as 0.07 nm and bonding angle of O–S–O as 110°, the molecular size in this direction is estimated to be approximately 0.4 nm. This is very close to the interlayer spacing of 0.4 nm for the first type of 2-NS·Mg–Al LDH. Therefore, the naphthalene ring of 2-NS⁻ is presumed to be oriented along an arrangement that is parallel to the brucite-like host layers of 2-NS·Mg–Al LDH, as shown in Fig. 4(a). On the other hand, the molecular size of 2-NS⁻ along the direction parallel to the planar structure is estimated to be approximately 1 nm using various bond parameters such as covalent radii and bonding angles of elements constituting 2-NS⁻. This size is smaller than the value (1.4 nm) of the interlayer spacing of another 2-NS·Mg–Al LDH type expected from the XRD peak position at the 2θ value of about 5°. The naphthalene ring of 2-NS⁻ is presumed to be oriented along a direction perpendicular to the brucite-like layers with the $-SO_3^-$ group attached to the host lattice, as shown in Fig. 4(b). The 2-NS⁻ is considered to contain both

activated and deactivated parts in the naphthalene ring structure, as shown in Fig. 1(a). Therefore, a deactivated part and an activated part in the naphthalene ring of a 2-NS⁻ are considered to be in an inversely-related configuration in the interlayer of Mg–Al LDH, as shown in Fig. 4(b). This is due to the π–π stacking interactions that are presumed to determine the configuration of 2-NS⁻ in the interlayer.

Furthermore, it was observed in the XRD patterns of the 2-NS·Mg–Al LDHs (Fig. 2) that the intensity of a diffraction peak at the 2θ value of about 5°, corresponding to $d = 1.87$ nm, increased with an increase in the 2-NS/Al mole ratio in the solution. With an increase in the intercalation of 2-NS⁻ in the interlayer of 2-NS·Mg–Al LDH, the π–π stacking interactions are presumed to cause a fairly regular arrangement of the intercalated 2-NS⁻.

3.2   Preparation of 2,6-NDS·Mg–Al LDH

2,6-NDS·Mg–Al LDHs were prepared at a constant pH of 10.0 by dropwise addition of Mg–Al solution to the 2,6-NDS–Na solutions at three different concentrations—0.5, 1.0 and 2.0 times as much as the stoichiometric quantity required by eq. (2), i.e., 2,6-NDS/Al mole ratio = 0.25, 0.5, and 1.0, respectively.

Table 3 shows that the sample prepared, 2,6-NDS·Mg–Al LDHs contained 2,6-NDS as well as Mg and Al at an Mg/Al mole ratio of 2.9. The 2,6-NDS/Al mole ratio in the sample increased with an increase in its ratio in the solution from 0.25 to 0.5; however, no further increase was observed during the increase in the ratio from 0.5 to 1.0. The intercalation of 2,6-NDS²⁻ was less than the 2,6-NDS/Al ratio of 0.5 that is required for the neutralisation of the entire positive charge of the host layer of Mg–Al LDH.

Figure 5 shows the XRD patterns of (a) CO_3·Mg–Al LDH and 2,6-NDS·Mg–Al LDHs prepared from solutions with the 2,6-NDS/Al mole ratios of (b) 0.25, (c) 0.5 and (d) 1.0. Although the XRD peaks of spectrum (b) were broader in comparison with those of CO_3·Mg–Al LDH, they were ascribed to hydrotalcite (JCPDS card 22–700). This indicates that the 2,6-NDS·Mg–Al LDH had a structure similar to Mg–

Table 3　Element analyses and mole ratios of Mg/Al and 2,6-NDS/Al for 2,6-NDS·Mg–Al LDHs prepared from solutions with 2,6-NDS/Al mole ratios of 0.25, 0.5 and 1.0.

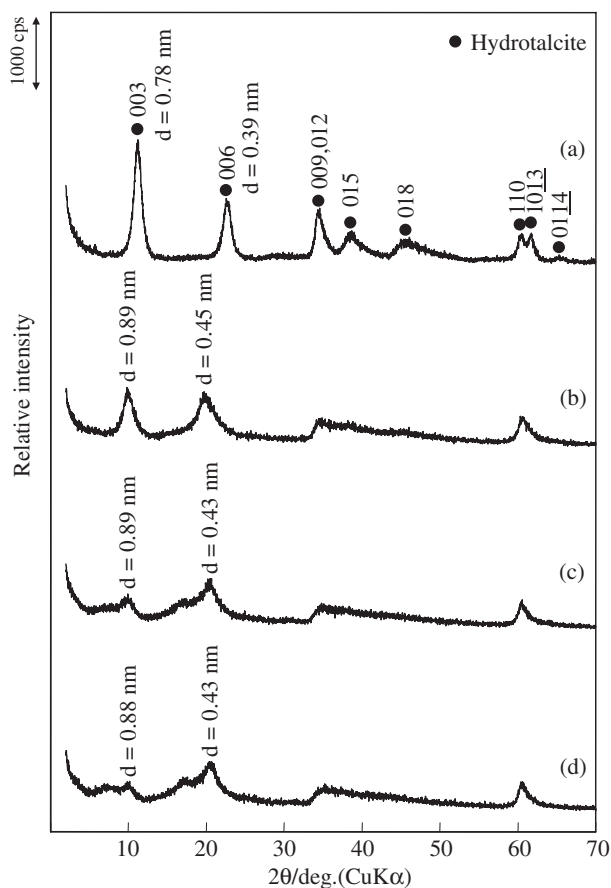| 2,6-NDS/Al mole ratio in solution	mass%			mole ratio	
	Mg	Al	2,6-NDS	Mg/Al	2,6-NDS/Al
0.25	20.4	7.8	20.6	2.9	0.25
0.5	18.0	6.9	29.3	2.9	0.40
1.0	17.9	6.8	26.3	2.9	0.36

Fig. 5　XRD patterns of (a) CO_3·Mg–Al LDH and 2,6-NDS·Mg–Al LDHs prepared from solutions with 2,6-NDS/Al mole ratios of (b) 0.25, (c) 0.5 and (d) 1.0.

Fig. 6　FT-IR spectra of (a) CO_3·Mg–Al LDH, (b) 2,6-NDS–Na_2 and 2,6-NDS·Mg–Al LDHs prepared from solutions with 2,6-NDS/Al mole ratios of (c) 0.25, (d) 0.5 and (e) 1.0.

Al LDH. The peaks corresponding to the d_{003} and d_{006} peaks of CO_3·Mg–Al LDH shown in Fig. 5(a) were observed at $10°$ and $20°$ (2θ) in Fig. 5(b), respectively, and the peak intensity decreased as 2,6-NDS^{2-} was introduced into the interlayers. This suggests that the 2,6-NDS·Mg–Al LDH has a basal spacing of approximately 0.9 nm caused by the intercalation of 2,6-NDS^{2-} in the interlayer of Mg–Al LDH. In the XRD patterns (c) and (d), it appears that the peak at about $10°$ (2θ) drastically reduced in intensity and was broadened significantly. It was also observed that the peak at around $20°$ (2θ) shifted slightly towards a higher angle but was almost unchanged in its intensity. Furthermore, the broad and weak peaks appeared at around $7°$ and $17°$ (2θ). Since the 2θ values larger than $30°$ in the XRD patterns (b) to (d) were analogous to those of hydrotalcite, it is confirmed that the 2,6-NDS·Mg–Al LDHs possess a basic lattice structure similar to Mg–Al LDH. The weakened and broadened band of XRD
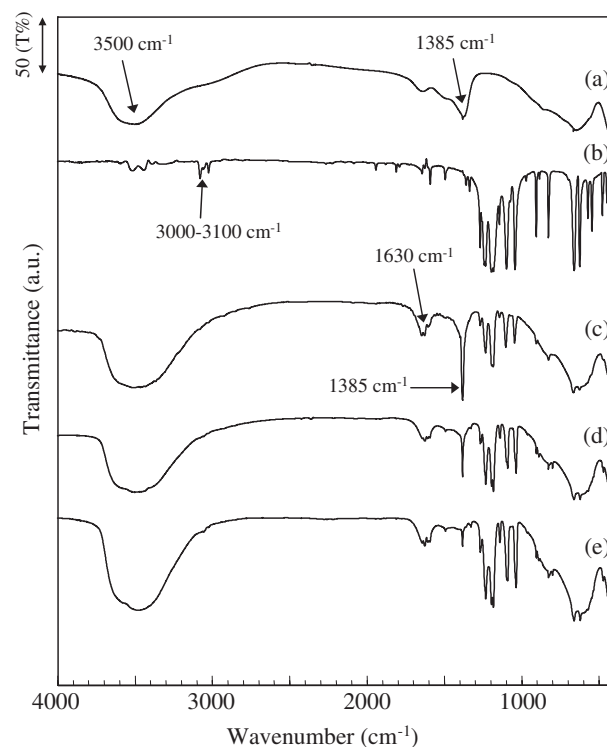
peaks spreading over 2θ values ranging from $6°$ to $11°$ are considered to reflect the varying basal spacings of 2,6-NDS·Mg–Al LDH with increasing 2,6-NDS/Al mole ratios in the crystal. This is probably caused by the various orientations of 2,6-NDS^{2-} in the interlayer. The XRD patterns of 2,6-NDS·Mg–Al LDHs were significantly different from those of 2-NS·Mg–Al LDHs in Fig. 2, although the difference between the molecular structures of 2-NS$^-$ and 2,6-NDS^{2-} lies in the number of $-SO_3^-$ groups arranged in the naphthalene ring—one in the former and two in the latter. This difference in the XRD patterns will be discussed later.

Figure 6 shows the FT-IR spectra of (a) CO_3·Mg–Al LDH, (b) 2,6-NDS–Na_2 and 2,6-NDS·Mg–Al LDHs prepared from solutions with 2,6-NDS/Al mole ratios of (c) 0.25, (d) 0.5 and (e) 1.0. The FT-IR spectra of 2,6-NDS·Mg–Al LDHs displayed absorption bands that are characteristic both to CO_3·Mg–Al LDH and 2,6-NDS–Na_2, suggesting that the samples prepared are Mg–Al LDHs intercalated with 2,6-NDS^{2-}. Analogously to the case of 2-NS$^-$, 2,6-NDS^{2-} remains unchanged in the interlayer. OH$^-$ is also considered to participate in the intercalation from the absorption band
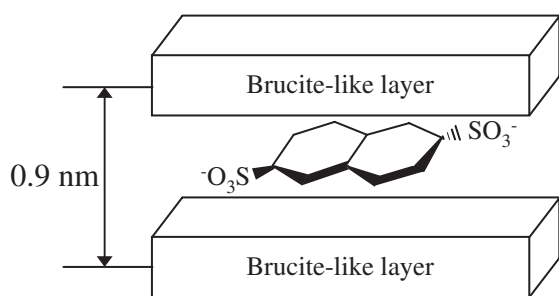
Fig. 7 Orientation of the naphthalene ring of 2,6-NDS²⁻ along a direction parallel to the brucite-like layers of 2,6-NDS·Mg–Al LDH.

observed at 1385 cm⁻¹ due to the O–H bending vibration in the 2,6-NDS·Mg–Al LDHs as well as 2-NS·Mg–Al LDHs.

The XRD patterns of 2,6-NDS·Mg–Al LDH shown in Fig. 5(b) suggest that 2,6-NDS²⁻ has been intercalated according to a simple configuration, which corresponds to the basal spacing of 0.9 nm. Considering the brucite-like layer thickness of 0.48 nm,[23] the interlayer spacing is calculated to be approximately 0.4 nm. The 2,6-NDS²⁻ contains a planar-structured naphthalene ring as well as 2-NS⁻ in its structure. The molecular size of 2,6-NDS²⁻ in the direction perpendicular to the planar structure is calculated to be approximately 0.4 nm similar to the 2-NS⁻ anion. This value is determined from the sizes of the –SO₃⁻ groups and is very close to the interlayer spacing. This leads to a speculation that the naphthalene ring of 2,6-NDS²⁻ is oriented along a direction parallel to the brucite-like layers, as shown in Fig. 7. The widely spreading and weakened X-ray diffraction peaks at 2θ values ranging from 6° to 11° in Figs. 5(c) and (d) suggest that the irregular arrangement of 2,6-NDS²⁻ in the LDH interlayers leads to the stacking of the host layers with irregularly varying basal spacing. The two –SO₃⁻ groups in 2,6-NDS²⁻ interact electrostatically with the positive charge of the brucite-like host layer. The extremities of the individual anions are pinned up to either side of the interlayers, and their mobility is limited as compared with 2-NS⁻. Furthermore, the uniformly deactivated naphthalene ring in 2,6-NDS²⁻ repels other rings electrostatically. Owing to these reasons, 2,6-NDS²⁻ is assumed to orient in an irregular manner in the interlayer of Mg–Al LDH with the increase in the 2,6-NDS/Al mole ratio. From Table 3, the intercalation of 2,6-NDS²⁻ was calculated to be approximately 80% of the expected value. The disturbed configuration of 2,6-NDS²⁻ in the interlayer of Mg–Al LDH is expected to impart a negative effect on the intercalation. In contrast, in 2-NS⁻, one –SO₃⁻ group is electrostatically fixed on one side of the interlayer in Mg–Al LDH. The naphthalene ring appears to be noticeably mobile in the interlayer. Therefore, the π–π stacking interactions between the naphthalene rings are considered to actively contribute to the well-ordered configuration of 2-NS⁻ in the interlayers.

In this study, the Mg–Al LDHs modified with 2-NS⁻ (naphthalene ring containing one –SO₃⁻ group) or 2,6-NDS²⁻ (naphthalene ring containing two –SO₃⁻ groups) were prepared and the products were characterised using XRD and FT-IR methods. These aromatic-modified Mg–Al LDHs are found to uptake bisphenol A and diethyl phthalate

from an aqueous solution. The detailed evaluation and discussion are being currently conducted and will be reported later.

4. Conclusions

(1) 2-NS·Mg–Al LDH or 2,6-NDS·Mg–Al LDH, which had 2-NS⁻ or 2,6-NDS²⁻ intercalated in the interlayer of Mg–Al LDH, was prepared by dropwise addition of a mixed aqueous solution of Mg(NO₃)₂ and Al(NO₃)₃ in the Mg/Al mole ratio of 3.0 to an aqueous-ethanol solution of 2-NS–Na or to an aqueous solution of 2,6-NDS–Na₂ at a constant pH of 10.0, and then being kept standing at 30°C for 1 h. The intercalated 2-NS⁻ or 2,6-NDS²⁻ maintained its intrinsic molecular structure in the interlayer of Mg–Al LDH.

(2) It was concluded from the result of the XRD analysis that 2-NS·Mg–Al LDH had two basal spacings of approximately 1.9 and 0.9 nm, respectively. It was most likely that 2-NS⁻ was intercalated in the interlayer of Mg–Al LDH in two types of orientations. It was considered that the naphthalene ring of 2-NS⁻ was oriented along a direction parallel and perpendicular to the brucite (Mg(OH)₂)-like layers of Mg–Al LDH.

(3) The 2-NS/Al mole ratio in the 2-NS·Mg–Al LDH increased with an increase in the 2-NS/Al mole ratio in solution, and the interlayer of Mg–Al LDH was intercalated with 2-NS⁻ to almost full accommodation for the neutralisation of the positive charge of the host lattice at the 2-NS/Al mole ratio of 2.0 in solution.

(4) The XRD patterns of 2,6-NDS·Mg–Al LDH exhibited very weak, broadened peaks corresponding to the basal spacings at 2θ ranging from 6° to 11°, suggesting an irregular arrangement of 2,6-NDS²⁻ in the Mg–Al LDH interlayers. This is attributed to the limited mobility of the 2,6-NDS²⁻ resulting from the pin-up of the anions at the two –SO₃⁻ groups to either side of the interlayer. The intercalation with 2,6-NDS²⁻ unlike in 2-NS⁻, was approximately 80% of the value expected due to the charge balance on the Mg–Al LDH. The disordered configuration of 2,6-NDS²⁻ in the interlayer of Mg–Al LDH was presumed to restrict the intercalation.

REFERENCES

1) L. Ingram and H. F. W. Taylor: Mineral Mag. **36** (1967) 465–479.
2) S. Miyata: Clays Clay Miner. **31** (1983) 305–311.
3) F. Cavani, F. Trifiro and A. Vaccari: Catal. Today **11** (1991) 173–301.
4) T. Sato, T. Wakabayashi and M. Shimada: Ind. Eng. Chem. Prod. Res. Dev. **25** (1986) 89–92.
5) T. Sato, S. Onai, T. Yoshioka and A. Okuwaki: J. Chem. Tech. Biotechnol. **57** (1993) 137–140.
6) L. M. Parker, N. B. Milestone and R. H. Newman: Ind. Eng. Chem. Res. **34** (1995) 1196–1202.
7) T. Kameda, Y. Miyano, T. Yoshioka, M. Uchida and A. Okuwaki: Chem. Lett. **29** (2000) 1136–1137.
8) Y. W. You, H. T. Zhao and G. F. Vance: Environ. Technol. **22** (2001) 1447–1457.
9) T. Kameda, T. Yoshioka, M. Uchida, Y. Miyano and A. Okuwaki: Bull. Chem. Soc. Jpn. **75** (2002) 595–599.
10) C. D. Nava, M. S. Rios and M. T. Olguin: Sep. Sci. Technol. **38** (2003) 131–147.
11) T. Kameda, F. Yabuuchi, T. Yoshioka, M. Uchida and A. Okuwaki:

Water Res. **37** (2003) 1545–1550.

12) T. Kameda, T. Yoshioka, T. Mitsuhashi, M. Uchida and A. Okuwaki: Water Res. **37** (2003) 4045–4050.

13) T. Kameda, T. Yoshioka, T. Hoshi, M. Uchida and A. Okuwaki: Sep. Purification Tech. **42** (2005) 25–29.

14) E. Narita, T. Yamagishi and T. Tonai: Nippon Kagaku Kaishi **1992** (1992) 291–296.

15) M. C. Hermosin, I. Pavlovic, M. A. Ulibarri and J. Cornejo: Wat. Res. **30** (1996) 171–177.

16) I. Pavlovic, M. A. Ulibarri, M. C. Hermosin and J. Cornejo: Fresenius Envir. Bull. **6** (1997) 266–271.

17) N. Takahashi, K. Kosuge, T. Nakai and Y. Sato: Mizu Kankyou Gakkaishi **25** (2002) 553–558.

18) J. Orthman, H. Y. Zhu and G. Q. Lu: Sep. Purification Tech. **31** (2003) 53–59.

19) T. Kameda, M. Saito and Y. Umetsu: J. Alloys Compd. **402** (2005) 46–52.

20) T. Kameda, S. Saito and Y. Umetsu: Sep. Purification Tech. **47** (2005) 20–26.

21) K. Ueno: *Kirēto Tekiteihou*, (Nankoudou, Tokyo, 1967).

22) S. P. Newman and W. Jones: New J. Chem. **22** (1998) 105–115.

23) S. Miyata: Clays Clay Miner. **23** (1975) 369–375.

24) S. Miyata, T. Kumura, H. Hattori and K. Tanabe: Nippon Kagaku Zasshi **92** (1971) 514–519.

25) J. T. Kloprogge, D. Wharton, L. Hickey and R. L. Frost: Amer. Miner. **87** (2002) 623–629.